Tuijin Jishu/Journal of Propulsion Technology
ISSN: 1001-4055
Vol. 45 No. 3 (2024)

Mathematical Strategies Using Differential Equations for Controlling Nipah Virus and COVID-19: A Combined Study

Rajan Kumar Dubey[1] ,Rajesh Pandey[2]
Department of Mathematics and Statistic, Deen Dayal Upadhyaya Gorakhpur University, Gorakhpur, U.P.(India), 273009

Abstract:- This study explores the use of differential equation-based mathematical models to understand and control the spread of Nipah virus (NiV) and COVID-19. By examining transmission dynamics and key epidemiological parameters, the research evaluates the effectiveness of intervention strategies such as vaccination, quarantine, social distancing, and public health campaigns. The analysis highlights the high fatality rate and zoonotic transmission of NiV compared to the high transmissibility and socioeconomic impact of COVID-19. Insights from these models aim to inform strategic interventions for mitigating future outbreaks, drawing comparisons to enhance public health responses to both pathogens.

Keywords*:* Nipah virus (NiV), COVID-19, Vaccination efficacy, Outbreaks, Transmission.

1. Introduction

The emergence of novel infectious diseases presents significant challenges to global public health. Two such pathogens, the Nipah virus (NiV) and the coronavirus disease 2019 (COVID-19), have caused substantial morbidity and mortality. The Nipah virus, first identified in Malaysia in 1998, is a zoonotic pathogen with a high fatality rate, often causing severe respiratory and neurological symptoms [1][2]. In contrast, COVID-19, caused by the severe acute respiratory syndrome coronavirus (SARS-CoV-2), emerged in late 2019 and rapidly escalated into a global pandemic, characterized by its high transmissibility and significant socioeconomic impact [3-5].

Mathematical modeling, particularly through differential equations, has proven to be an invaluable tool in understanding and controlling the spread of infectious diseases [6-7]. This study, titled "Mathematical Strategies Using Differential Equations for Controlling Nipah Virus and COVID-19: A Combined Study," aims to develop and analyze mathematical models that can effectively describe the transmission dynamics of both Nipah virus and COVID-19. By leveraging these models, we seek to propose strategic interventions that could mitigate the spread of these pathogens.

Nipah virus is a highly lethal pathogen with an estimated case fatality rate of $40\,\%\ to\ 75\,\%$, varying by outbreak and health care context [8-10]. The primary mode of transmission is through direct contact with infected animals or their bodily fluids, and human-to-human transmission has also been documented [11]. Previous outbreaks have highlighted the virus's potential to cause severe outbreaks with high mortality rates, necessitating robust control measures [12]. Mathematical models for NiV have primarily focused on understanding its transmission dynamics and evaluating the impact of various intervention strategies.

COVID-19 has reshaped the modern world, leading to unprecedented public health measures and global scientific collaboration. The disease is primarily transmitted through respiratory droplets, with secondary transmission occurring via fomites and close contact [13-14]. The rapid spread of SARS-CoV-2 has prompted extensive research into its epidemiological characteristics and control mechanisms. Mathematical models have been crucial in forecasting infection rates, evaluating the effectiveness of interventions such as social distancing, quarantine, and vaccination, and informing public health policies [15].

Differential equations provide a framework for modeling the dynamic behavior of infectious diseases by describing the rate of change of populations within a system. For infectious disease modeling, compartmental models such as the Susceptible-Infectious-Recovered (SIR) model and its variants are widely used [16]. These models divide the population into compartments and use differential equations to describe the flow of individuals between compartments based on disease transmission rates, recovery rates, and other factors. In the context of NiV and COVID-19, differential equations can capture the complexities of transmission dynamics, including the effects of latency periods, varying contact rates, and heterogeneous mixing patterns within populations [17-18]. By fitting these models to epidemiological data, we can estimate key parameters, predict future outbreaks, and evaluate the potential impact of different control strategies [19-20].

In this research article with the help of mathematical models using differential equations that we represent the transmission dynamics of Nipah virus and COVID-19. We estimate the critical parameters influencing the spread of both viruses using available epidemiological data. Also we analyze the effectiveness of various intervention strategies, including vaccination, quarantine, social distancing, and public health campaigns, in controlling the spread of these diseases. We compare and contrast the transmission dynamics and control measures of NiV and COVID-19, identifying similarities and differences that could inform future outbreak response strategies.

2. Mathematical Model

We formulate a mathematical model to describe the transmission dynamics of the Nipah virus (NiV) or COVID-19. The progression of NiV or COVID-19 within the population is simplified into four, representing different groups of individuals. S denotes Individuals vulnerable to contracting NiV or COVID-19, E denotes individuals who have come into contact with NiV or COVID-19 but are not yet infectious, I denotes individuals who are infected with NiV or COVID-19 and capable of transmitting the virus. R denotes individuals who have recovered from NiV or COVID-19 and are immune.

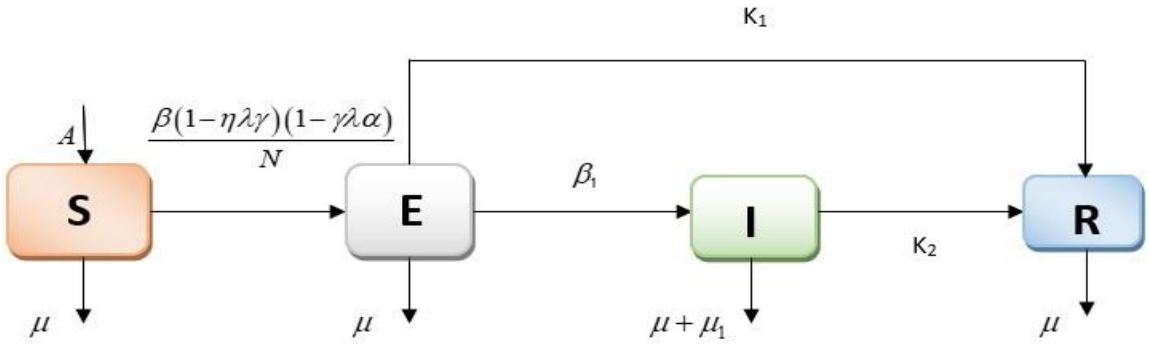

Figure 1: Flow diagram for a model system (2.1) to (2.4).

$$\frac{dS}{dt} = A - \frac{\beta\,(1-\eta\,\lambda\,\gamma)(1-\gamma\,\lambda\,\alpha)}{N} SI - \mu\,S, \qquad \ldots(2.1)$$

$$\frac{dE}{dt} = \frac{\beta\,(1-\eta\,\lambda\,\gamma)(1-\gamma\,\lambda\,\alpha)}{N} SI - \beta_1 E - k_1 E - \mu\,E, \qquad \ldots(2.2)$$

$$\frac{dI}{dt} = \beta_1 E - k_2\,I - \mu_1\,I - \mu\,I, \qquad \ldots(2.3)$$

$$\frac{dR}{dt} = k_1\,E + k_2\,I - \mu\,R \qquad \ldots(2.4)$$

with the condition that

$$S(0),\ E(0),\ I(0) \text{ and } R(0) \geq 0$$

where, $N = S + E + I + R$.

This approach not only provides insights into the spread of NiV but also serves as a foundation for comparing and contrasting with COVID-19 transmission dynamics. By leveraging these mathematical strategies, we aim to propose effective intervention measures to control the spread of both Nipah virus and COVID-19.

Table 1: Table of Description

Variable and Parameter	Description
S	Fraction of susceptible case
E	Fraction of exposed case
I	Fraction of infected case
R	Fraction of recovered case
A	Recruitment Rate
β	Rate of effective transmission of Nipah Virus
β_1	Progression rate of infection
μ	Natural death rate
μ_1	Death rate due to disease
k_1	Recovery rate of exposed individuals due to awareness
k_2	Recovery rate of infectious individuals due to treatment
η	Number of quarantine individuals
δ	Availability of isolation centers
γ	Enhanced personal hygiene due to public enlightenment
α	Rate of public enlightenment
λ	Surveillance coverage

Let us now outline Equations (2.1)-(2.4) of our model in detail. We begin with the birth rate, represented by A, which indicates the influx of individuals becoming susceptible. From this, we subtract the term μS, accounting for the natural death rate within the susceptible population, as shown in Equation (2.1).

In this equation, the second term $\frac{\beta\,(1-\eta\,\lambda\,\gamma)(1-\gamma\,\lambda\,\alpha)}{N} SI$ quantifies the rate at which susceptible individuals become exposed, as illustrated in Figure 1. This same term is also added in Equation (2.2), where it represents the new exposures. In addition to this, Equation (2.2) includes the terms μE, and $k_1 E$ which denote the rates at which exposed individuals die from natural causes (not necessarily NiV or COVID-19), transition to the infected category, and recover, respectively.

3. Model analysis

3.1. Feasible solution

The feasible solution set, which remains positively invariant under the model, is describe by

$$\Omega = \{ (S, E, I, R) \in R_+^4 : S + E + I + R = N \}$$

It will be demonstrated from Equations (2.1) to (2.4) that the region remains positively invariant. The total population is expressed as $N = S + E + I + R$.

By adding Equations (2.1) to (2.4), we get

For constant parameters A, v, v_s and μ.

$$\frac{dN}{dt} = A - \mu_1 I - \mu N \qquad \text{...(3.1)}$$

Thus, from above it is clear that if the system is disease free $(i.e. I = 0)$ then equation (3.1) takes the form as

$$\frac{dN}{dt} = A - \mu N \quad \text{...(3.2)}$$

3.2. Methods of solution

Above equation (3.2) can be written as

$$\frac{dN}{dt} + \mu N = A$$

This is a linear differential equation of oder one and degree one.

Compare above equation with $\frac{dN}{dt} + PN = Q$ then $P = \mu \ and \ Q = A$.

Integrating factors $e^{\mu t}$, its solution is given by $N(t) = \frac{A}{\mu} + Ce^{\mu t}$.

At $t = 0$

$$N(0) = \frac{A}{\mu} + C$$

Thus, $$C = N(0) - \frac{A}{\mu}$$

Hence the solution is given by

$$N(t) = \frac{A}{\mu} + \left\{N(0) - \frac{A}{\mu}\right\} e^{\mu t}$$

When $t \to \infty \ then \ N(t) \geq \frac{A}{\mu}$. Therefore, Ω is positively invariant.

3.3. Existence of steady states of the system

The equilibrium points of the system can be found by setting the rate of change of all compartments to zero.

Thus, $\frac{dS}{dt} = \frac{dE}{dt} = \frac{dI}{dt} = \frac{dR}{dt} = 0$.

From (2.1) to (2.4), we have

$$A - \frac{\beta(1-\eta\lambda\gamma)(1-\gamma\lambda\alpha)}{N} SI - \mu S = 0, \quad \text{...(3.3)}$$

$$\frac{\beta(1-\eta\lambda\gamma)(1-\gamma\lambda\alpha)}{N} SI - r_1 E = 0, \quad \text{...(3.4)}$$

$$\beta_1 E - r_2 I = 0, \quad \text{...(3.5)}$$

$$k_1 E + k_2 I - \mu R = 0 \quad \text{...(3.6)}$$

where $r_1 = \beta_1 + k_1 + \mu \ \ and \ \ r_2 = \mu_1 + k_2 + \mu$.

From equation (3.5)

$$I = \frac{\beta_1 E}{r_2} \quad \text{...(3.7)}$$

Using these value in (3.4), we get

$$\frac{\beta(1-\eta\lambda\gamma)(1-\gamma\lambda\alpha)}{N} S.\frac{\beta_1 E}{r_2} - r_1 E = 0$$

or, $$\left(\frac{\beta\beta_1(1-\eta\lambda\gamma)(1-\gamma\lambda\alpha)}{N r_2} S - r_1\right) E = 0$$

From above, either $E = 0 \ or \ \frac{\beta\beta_1(1-\eta\lambda\gamma)(1-\gamma\lambda\alpha)}{N r_2} S - r_1 = 0.$

$$S = \frac{r_1 r_2 N}{\beta\beta_1(1-\eta\lambda\gamma)(1-\gamma\lambda\alpha)} \quad \text{...(3.8)}$$

Similarly we can find the value of E, I and R which is given as

$$E = \frac{A\beta\beta_1 r_2(1-\eta\lambda\gamma)(1-\gamma\lambda\alpha) - r_1 r_2^2 \mu N}{\beta\beta_1 r_1 r_2(1-\eta\lambda\gamma)(1-\gamma\lambda\alpha)} \quad \text{...(3.9)}$$

$$I = \frac{\beta\beta_1\,(1-\eta\,\lambda\,\gamma)(1-\gamma\,\lambda\,\alpha)-r_1\,r_2\,\mu\,N}{\beta\;r_1\,r_2\,(1-\eta\,\lambda\,\gamma)(1-\gamma\,\lambda\;\alpha)} \quad ...(3.10)$$

and $R = \frac{A\beta\;\beta_1\,k_1\,r_2\,(1-\eta\,\lambda\,\gamma)(1-\gamma\,\lambda\;\;\alpha)-k_1\,r_1\,r_2^2\,\mu\,N+A\beta\;\beta_1^2\,k_2(1-\eta\,\lambda\,\gamma)(1-\gamma\,\lambda\;\alpha)-\beta_1\,k_2\,r_1\,r_2\,\mu\,N}{\beta\;r_1\,r_2\,(1-\eta\,\lambda\,\gamma)(1-\gamma\,\lambda\;\alpha)}$ ...(3.11)

Conversely, when $E = 0$, Equation (3.7) gives us $I = 0$. Similarly, for these values, Equation (3.6) results in $R = 0$. Consequently, from Equation (3.3), we obtain $S = A$. Therefore, the disease-free equilibrium (DFE) point is $\left(\frac{A}{\mu}, 0, 0, 0\right)$ and the endemic equilibrium point is (S^*, E^*, I^*, R^*), where:

$$S^* = \frac{r_1 r_2\,N}{\beta_1\,T},$$

$$E^* = \frac{A\,\beta_1\,r_2\,T - r_1\,r_2^2\,\mu\,N}{\beta\,r_1 r_2\,T},$$

$$I^* = \frac{A\beta_1\,T - r_1\,r_2\,\mu\,N}{r_1 r_2\,T} \quad \text{and}$$

$$R^* = \frac{A\beta_1\,k_1\,r_2\,T - k_1 r_1\,r_2^2\,\mu\,N + A\beta_1^2\,k_2 T - \beta_1 k_2\,r_1 r_2\,\mu\,N}{\beta_1\,r_1\,r_2\,T}$$

Where, $T = \beta\,(1-\eta\,\lambda\,\gamma)(1-\gamma\,\lambda\;\alpha)$.

3.4. Basic reproductive number

The basic reproduction number, R_0, quantifies the potential for disease transmission within a population. Mathematically, R_0 is a threshold parameter that indicates the stability of a disease-free equilibrium and relates to the epidemic's peak and final size. It represents the expected number of secondary infections caused by a single primary case in a fully susceptible population. If R_0 is less than 1, introduced infected individuals will, on average, fail to replace themselves, preventing the disease from spreading. Conversely, if R_0 exceeds 1, the number of infected individuals will grow with each generation, leading to disease spread. While $R_0$is crucial for determining whether a diseases can invade a fully susceptible population, it may become less accurate as conditions change during the spread. Nonetheless, in many disease transmission models, the peak prevalence of infected hosts and the epidemic's final size both increase with R_0, making it a valuable metric for assessing disease spread.

The new infections come from the term involving β in the equation for E:

$$F = \begin{bmatrix} \frac{\beta\,(1-\eta\,\lambda\,\gamma)(1-\gamma\,\lambda\,\alpha)\}}{N} SI \\ 0 \end{bmatrix}$$

The transition terms include all other terms that do not represent new infections:

$$V = \begin{bmatrix} \beta_1\,E + k_1\,E + \mu\,E \\ -k_2\,I + \mu_1\,I + \mu\,I \end{bmatrix}$$

The Jacobian matrices of F and V are calculated at the disease-free equilibrium (DFE), where $S = N,\ E = 0,$ $I = 0\ and\ R = 0$.

$$J_F = \begin{bmatrix} \frac{\partial F_1}{\partial E} & \frac{\partial F_1}{\partial E} \\ \frac{\partial F_2}{\partial E} & \frac{\partial F_2}{\partial E} \end{bmatrix}$$

$$= \begin{bmatrix} 0 & \frac{\beta\,(1-\eta\,\lambda\,\gamma)(1-\gamma\,\lambda\,\alpha)\}}{N} S \\ 0 & 0 \end{bmatrix}$$

$$= \begin{bmatrix} 0 & \beta\,(1-\eta\,\lambda\,\gamma)(1-\gamma\,\lambda\,\alpha) \\ 0 & 0 \end{bmatrix}$$

Now,

$$J_v = \begin{bmatrix} \frac{\partial V_1}{\partial E} & \frac{\partial V_1}{\partial E} \\ \frac{\partial V_2}{\partial E} & \frac{\partial V_2}{\partial E} \end{bmatrix}$$

$$= \begin{bmatrix} \beta_1 + k_1 + \mu & \beta\,(1-\eta\,\lambda\,\gamma)(1-\gamma\,\lambda\,\alpha) \\ -\beta_1 & k_2 + \mu_1 + \mu \end{bmatrix}$$

The next-generation matrix is

$$K = J_F\, J_V^{-1} \qquad \text{...(3.12)}$$

$$= \begin{bmatrix} \frac{1}{\beta_1 + k_1 + \mu} & 0 \\ \frac{\beta_1}{(\beta_1 + k_1 + \mu)(k_2 + \mu_1 + \mu)} & \frac{1}{k_2 + \mu_1 + \mu} \end{bmatrix}$$

Using the value of J_F and J_V^{-1} in equation (3.12), we get

Now,

$$K = \begin{bmatrix} 0 & \frac{\beta\,\beta_1\,(1-\eta\,\lambda\,\gamma)(1-\gamma\,\lambda\,\alpha}{(\beta_1 + k_1 + \mu)(k_2 + \mu_1 + \mu)} \\ 0 & 0 \end{bmatrix}.$$

The basic reproductive number R_0 is the largest eigenvalue (spectral radius) of the matrix K. Here, it is simply the value in the matrix :

$$R_0 = \frac{\beta\,\beta_1\,(1-\eta\,\lambda\,\gamma)(1-\gamma\,\lambda\,\alpha}{(\beta_1 + k_1 + \mu)(k_2 + \mu_1 + \mu)}.$$

Thus, the basic reproductive number R_0 is :

$$R_0 = \frac{\beta\,\beta_1\,(1-\eta\,\lambda\,\gamma)(1-\gamma\,\lambda\,\alpha}{(\beta_1 + k_1 + \mu)(k_2 + \mu_1 + \mu)}. \qquad \text{...(3.13)}$$

3.5. Stability analysis

Mathematical models are becoming increasingly complex as they incorporate higher degrees of nonlinearity to address real-world problems. Finding explicit solutions for these models is nearly impossible. While numerical simulations can provide good approximate solutions with fixed parameters, the general solution may remain elusive. In such cases, stability analysis is a valuable tool to understand the behavior of the solutions. Stability analysis can effectively predict the long-term behavior of model solutions. Generally, two types of stability analysis are widely used: local and global. Local stability focuses on the behavior of the model solution near an equilibrium point, whereas global stability describes the solution's behavior across the entire domain.

3.5.1. Local stability analysis

In this section, we aim to demonstrate that the DFE point is locally stable using the following theorem

Theorem 1. *The disease free equilibrium $E_{\{DFE\}}$ of the system (2.1) to (2.4) is locally asymptotically stable if $R_0 < 1$ and unstable if $R_0 > 1$.*

Proof. First we determine the Jacobian Matrix at DFE. The Jacobian matrix J of the system at any point (S, E, I, R) is derived by taking the partial derivatives of each equation with respect to each variable.

$$J_F = \begin{bmatrix} \frac{\partial f_1}{\partial S} & \frac{\partial f_1}{\partial E} & \frac{\partial f_1}{\partial I} & \frac{\partial f_1}{\partial R} \\ \frac{\partial f_2}{\partial E} & \frac{\partial f}{\partial E} & \frac{\partial f_2}{\partial E} & \frac{\partial f}{\partial E} \\ \frac{\partial f_3}{\partial S} & \frac{\partial f_3}{\partial E} & \frac{\partial f_3}{\partial I} & \frac{\partial f_3}{\partial R} \\ \frac{\partial f_4}{\partial S} & \frac{\partial f_4}{\partial E} & \frac{\partial f_4}{\partial I} & \frac{\partial f_4}{\partial R} \end{bmatrix}$$

Evaluating the partial derivatives at the DFE $(S_0,\ E_0,\ I_0,\ R_0) = (N, 0, 0, 0)$

$$J_F = \begin{bmatrix} -\mu & 0 & -\beta\,(1-\eta\,\lambda\,\gamma)(1-\gamma\,\lambda\ \alpha) & 0 \\ 0 & -(\beta_1 + k_1 + \mu_{1)} & \beta\,(1-\eta\,\lambda\,\gamma)(1-\gamma\,\lambda\ \alpha) & 0 \\ 0 & -(k_2 + \mu_1 + \mu) & -(k_2 + \mu_1 + \mu) & 0 \\ 0 & k_1 & k_2 & -\mu \end{bmatrix}$$

To determine the local stability of the DFE, we need to find the eigenvalues of the Jacobian matrix. The DFE is locally asymptotically stable if all the eigenvalues have negative real parts.

Let us solve for the eigenvalues of J.

$$|(J - \lambda' I| = 0 \quad \text{...(3.14)}$$

where I is an identity matrix and λ' is an eigen value.

$$\begin{bmatrix} -\mu - \lambda' & 0 & -\beta\,(1-\eta\,\lambda\,\gamma)(1-\gamma\,\lambda\;\alpha) & 0 \\ 0 & -(\beta_1 + k_1 + \mu_1) - \lambda' & \beta\,(1-\eta\,\lambda\,\gamma)(1-\gamma\,\lambda\;\alpha) & 0 \\ 0 & \beta_1 & -(k_2 + \mu_1 + \mu) - \lambda' & 0 \\ 0 & k_1 & k_2 & -\mu - \lambda' \end{bmatrix} = 0$$

This determinant leads to a characteristic polynomial. The eigenvalues can be determined by solving this polynomial equation. However, from the structure of the Jacobian matrix, we can observe that there are two eigenvalues that are straightforward $\lambda_1 = -\mu$ and $\lambda_4 = -\mu$ (from the first row/column and from the fourth row/column).

For the 2×2 submatrix involving E and I :

$$\begin{vmatrix} -(\beta_1 + k_1 + \mu_1) - \lambda & \beta\,(1-\eta\,\lambda\,\gamma)(1-\gamma\,\lambda\;\alpha) \\ \beta_1 & -(k_2 + \mu_1 + \mu) - \lambda' \end{vmatrix} = 0$$

Or, $[-(\beta_1 + k_1 + \mu_1) - \lambda][-(k_2 + \mu_1 + \mu) - \lambda'] - [\beta\,(1-\eta\,\lambda\,\gamma)(1-\gamma\,\lambda\;\alpha)]\beta_1 = 0$

Or, $[\,(\beta_1 + k_1 + \mu_1) + \lambda'][(k_2 + \mu_1 + \mu) + \lambda'] = \beta\,\beta_1\,(1-\eta\,\lambda\,\gamma)(1-\gamma\,\lambda\;\alpha)$

Solving this quadratic equation gives us the other two eigenvalues. The critical threshold R_0 can be inferred from the signs of these eigenvalues:

$$R_0 = \frac{\beta\,\beta_1\,(1-\eta\,\lambda\,\gamma)(1-\gamma\,\lambda\,\alpha}{(\beta_1 + k_1 + \mu)(k_2 + \mu_1 + \mu)} \quad \text{...(3.15)}$$

If $R_0 < 1$, the real parts of all eigenvalues are negative, and the DFE is locally asymptotically stable. If $R_0 > 1$, at least one eigenvalue has a positive real part, making the DFE unstable.

Therefore, the local stability analysis concludes that the DFE is locally asymptotically stable if $R_0 < 1$ and unstable if $R_0 > 1$.

3.5.2. Global stability analysis

We will verify the global stability of the model by applying the Lyapunov principle, which is based on the following lemma.

Lemma 1. *The Disease- free Equilibrium (DFE) of the system is globally asymptotically stable if* $R_0 < 1$. *If* $R_0 > 1$, *the DFE is unstable.*

Proof. As we know that the Disease-Free Equilibrium (DFE) is $(S, E, I, R) = (S_0, 0, 0, 0)$

Assuming a constant population size N the DFE is:

$$S_0 = \frac{A}{\mu},\; E = 0, I = 0 \text{ and } R = 0.$$

A common choice for a Lyapunov function in epidemiological models is $V = E + I$. This function is non-negative and zero only at the DFE.

Now, we find the time derivative of V.

$$\frac{dV}{dt} = \frac{dE}{dt} + \frac{dI}{dt}$$

$$\frac{dV}{dt} = \left(\frac{\beta(1-\eta\lambda\gamma)(1-\gamma\lambda\,\alpha)}{N} SI - (\beta + k_1 + \mu)E\right) - (\beta_1 E - (k_2 + \mu_1 + \mu)I)$$

$$= \frac{\beta(1-\eta\lambda\gamma)(1-\gamma\lambda\,\alpha)}{N} SI - (k_1 + \mu)E - (k_2 + \mu_1 + \mu)I$$

Now, we evaluate the Lyapunov derivatives at the DFE, $S = \frac{A}{\mu},\; E = 0,\; I = 0$ and $R = 0$:

$$\frac{dV}{dt} = \frac{\beta(1-\eta\lambda\gamma)(1-\gamma\lambda\,\alpha)}{N}.\frac{A}{\mu}I - (k_1 + \mu)E - (k_2 + \mu_1 + \mu)I$$

Simplifying, we get

$$\frac{dV}{dt} = \left(\frac{\beta(1-\eta\lambda\gamma)(1-\gamma\lambda\,\alpha)A}{\mu N} - (k_2 + \mu_1 + \mu)\right) I - (k_1 + \mu)E \qquad ...(3.16)$$

For the DFE to be globally asymptotically stable, $\frac{dV}{dt}$ must be non positive. This condition is satisfied if the coefficient of I is non-positive and E is always non positive.
Thus, we require

$$\frac{\beta(1-\eta\lambda\gamma)(1-\gamma\lambda\,\alpha)A}{\mu N} < (k_2 + \mu_1 + \mu). \qquad ...(3.17)$$

This condition is equivalent to $R_0 < 1$ where

$$R_0 = \frac{\beta\beta_1(1-\eta\lambda\gamma)(1-\gamma\lambda\,\alpha)A}{(\beta_1 + k_1 + \mu)(k_2 + \mu_1 + \mu)}. \qquad ...(3.18)$$

If $R_0 < 1$, then $\frac{dV}{dt} \leq 0$, indicating that the DFE is globally asymptotically stable.

Hence using Lyapunov function $V = E + I$ and its derivative, we conclude that the Disease- free Equilibrium (DFE) of the system is globally asymptotically stable if $R_0 < 1$. If

$R_0 > 1$, the DFE is unstable, and the disease will spread in the population.

4. Numerical simulation

We present numerical simulations of the proposed control problem, utilizing clinically approved values relevant to Bangladesh for Nipah virus in case I and COVID-19 of India in case II, as outlined in Table 2. Our primary goal is to examine and understand the impact of control parameters, specifically the number of quarantined individuals η and enhanced personal hygiene due to public awareness γ. Figures $(2)-(8)$ illustrate the numerical outcomes of the model for varying control parameters. Figure 2 depicts the typical behavior of the susceptible, exposed, infected, and recovered populations without any control measures for Nipah virus in Bangladesh. It reveals that the number of susceptible individuals decreases from the initial stage due to the diminishing nature of this compartment over time, with the exposed population exhibiting a similar trend.

Table 2: Table of Description

Parameter	Case I/ Reference	Case II/ Reference
A	4751 day^{-1}[21]	35542 day^{-1}[22]
β	0.75 day^{-1}[23]	0.75 day^{-1}[19]
β_1	0.60 day^{-1}[23]	0.60 day^{-1}[23]
μ	3.8642×10^{-5} [24]	3.8642×10^{-5} [20]
μ_1	0.76 day^{-1}[24]	0.8 day^{-1} [25]
k_1	0.15 day^{-1}[23]	0.15 day^{-1}[23]
k_2	0.09 day^{-1}[23]	0.09 day^{-1}[23]
η	0 [Assumed]	0 [Assumed]
δ	0.65 [23]	0.45 [25]
γ	0 [Assumed]	0 [Assumed]

α	0.90 [23]	0.85 [26]
λ	0.85 [23]	0.85 [23]

In this scenario, the contact rate significantly influences the spread of the disease throughout the population. Close observation of the infected compartment reveals that the number of infected individuals rises sharply in a short time from the initial state, reaching its peak within three days before gradually declining. This figure also shows that the number of recovered individuals increases steadily over time. When control measures are applied, changes in the compartment dynamics are observed, as illustrated in Figures (2)-(8).

It can be observed from Figure 3 ($\eta = 0$ and $\gamma = 0.25$) that the infected compartment behaves differently compared to the previous figure, indicating that when control parameters are applied, the number of infected individuals decreases to zero after approximately 27 days. In Figure 4 ($\eta = 0.50$ and $\gamma = 0.25$), the rate of decline increases, with the infected population reaching zero after about 17 days. In Figure 5 ($\eta = 0.75$ and $\gamma = 0.50$) the infected population reaches zero in approximately 13 days. Figures 6 and 7 ($\eta = 0.75$ and $\gamma = 1.0$) and ($\eta = 1.0$ and $\gamma = 0.75$) show that the infected population reaches zero after roughly 10 days. When considering ($\eta = 1.0$ and $\gamma = 1.0$) as shown in Figure 8, the infected population decreases to zero in 10 days. These graphs illustrate that the control parameters have a significant impact on the spread of the disease within the population. A higher control rate logically leads to a lower infection rate.

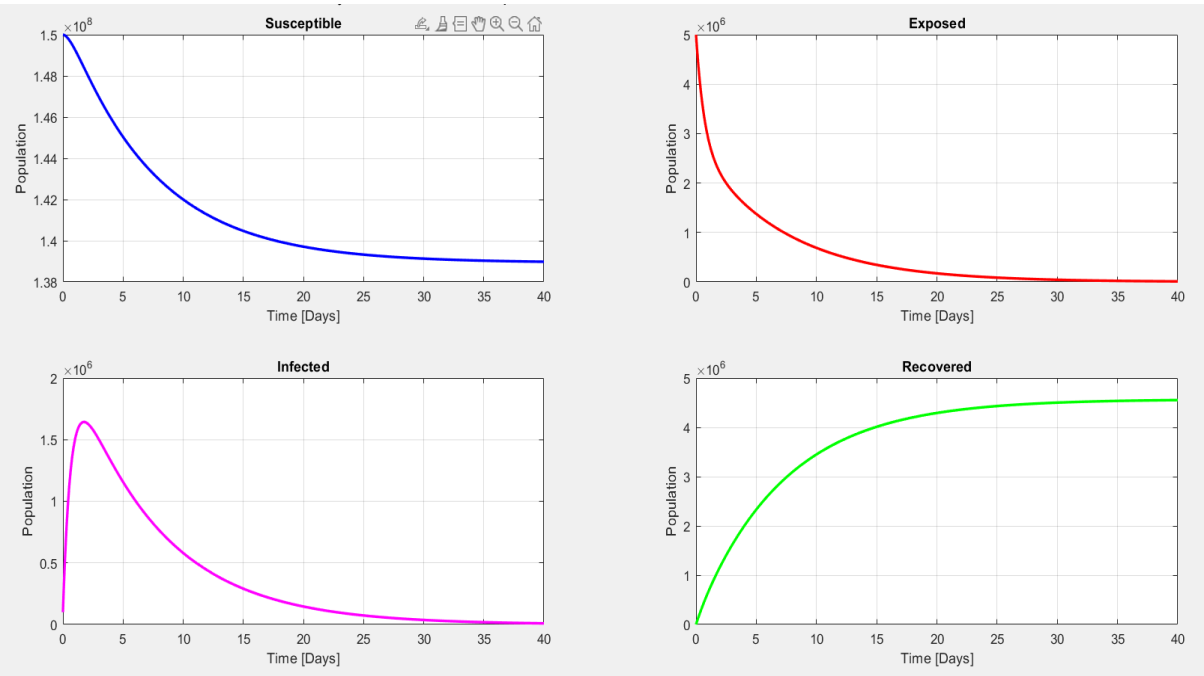

Figure 2: Dynamics of the compartments for the values of the control parameter $\eta = 0$ and $\gamma = 0$ with $R_0 = 0.71$.

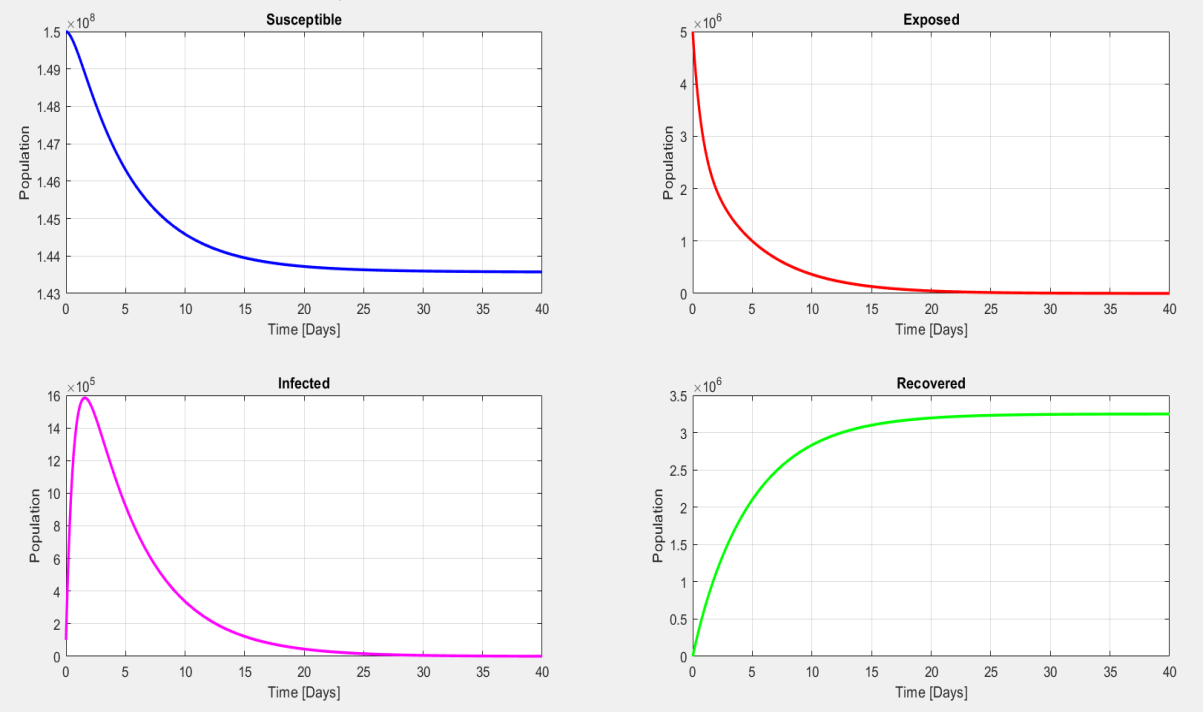

Figure 3: Dynamics of the compartments for the values of the control parameter $\eta = 0$ and $\gamma = 0.25$ with $R_0 = 0.51$.

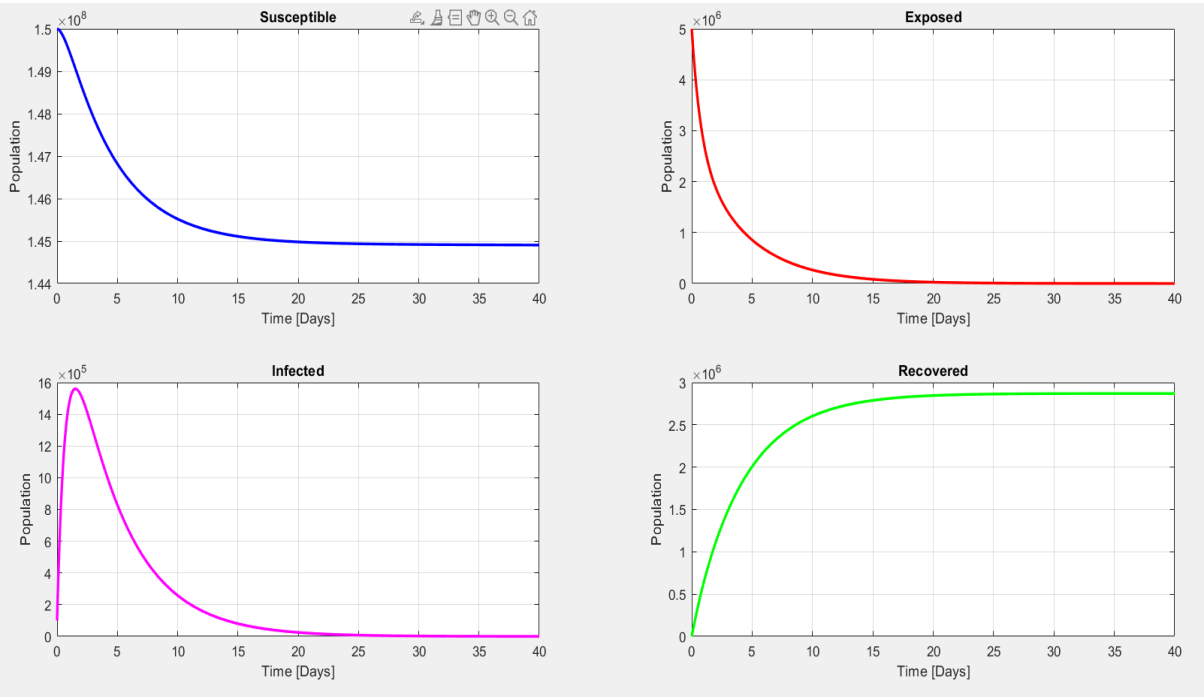

Figure 4: Dynamics of the compartments for the values of the control parameter $\eta = 0.50$ and $\gamma = 0.25$ with $R_0 = 0.41$.

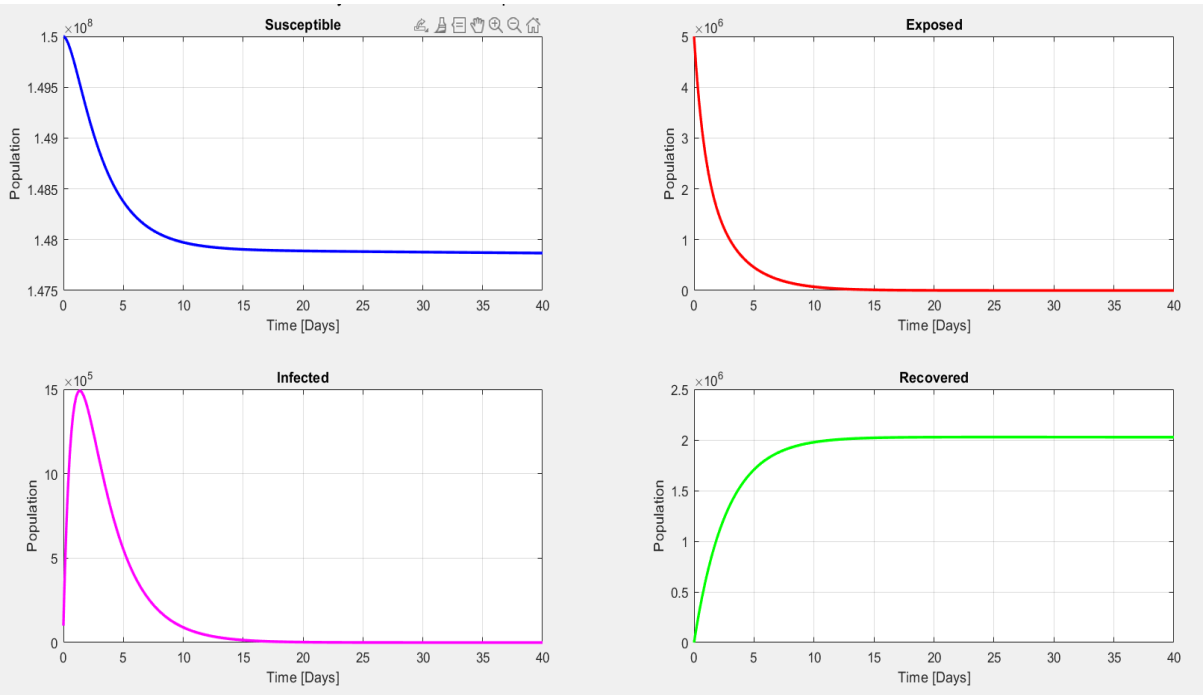

Figure 5: Dynamics of the compartments for the values of the control parameter $\eta = 0.75$ and $\gamma = 0.50$ with $R_0 = 0.25$.

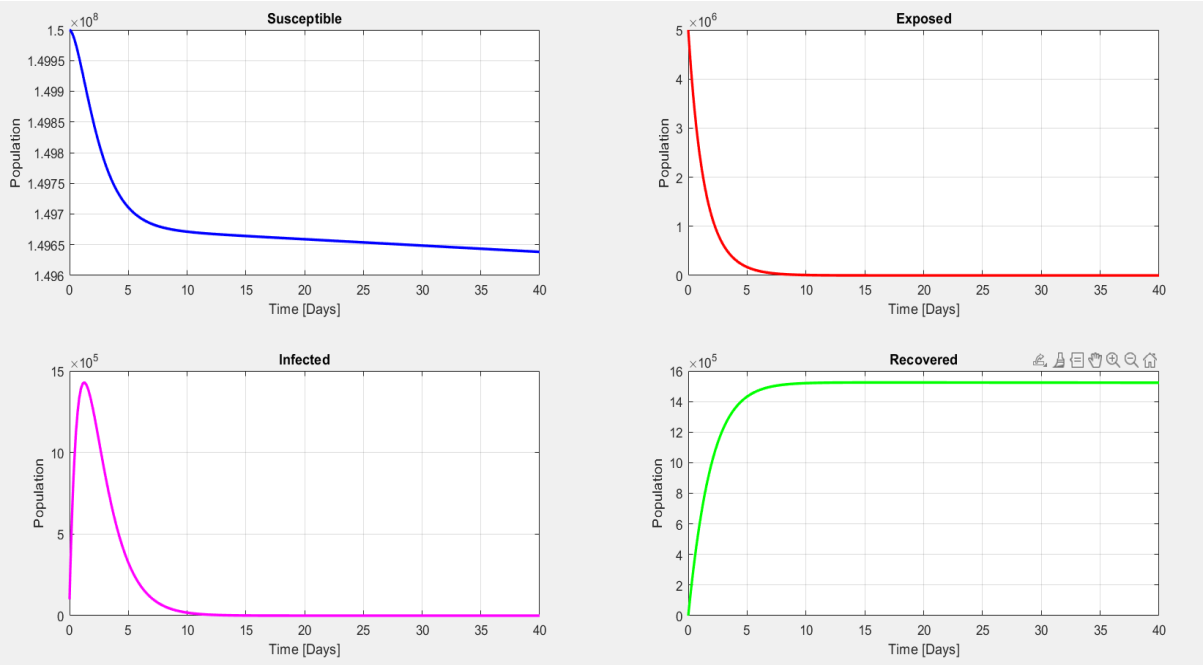

Figure 6: Dynamics of the compartments for the values of the control parameter $\eta = 0.75$ and $\gamma = 1.0$ with $R_0 = 0.10$.

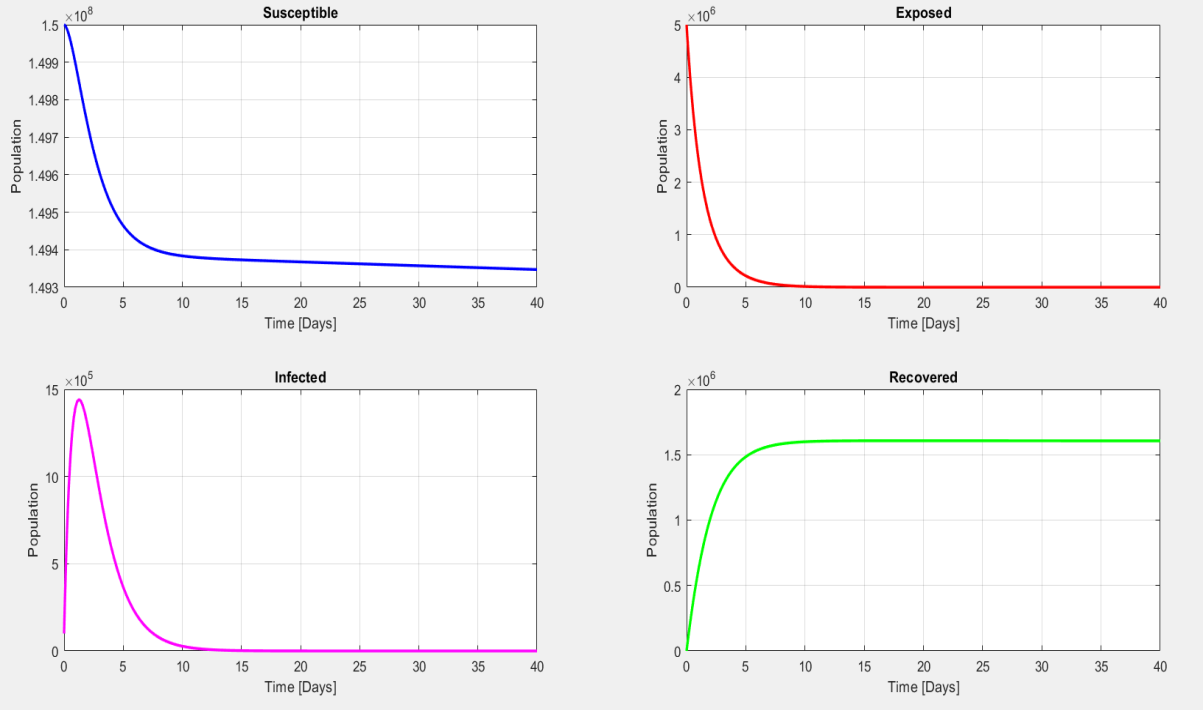

Figure 7: Dynamics of the compartments for the values of the control parameter $\eta = 1.0$ and $\gamma = 0.75$ with $R_0 = 0.15$.

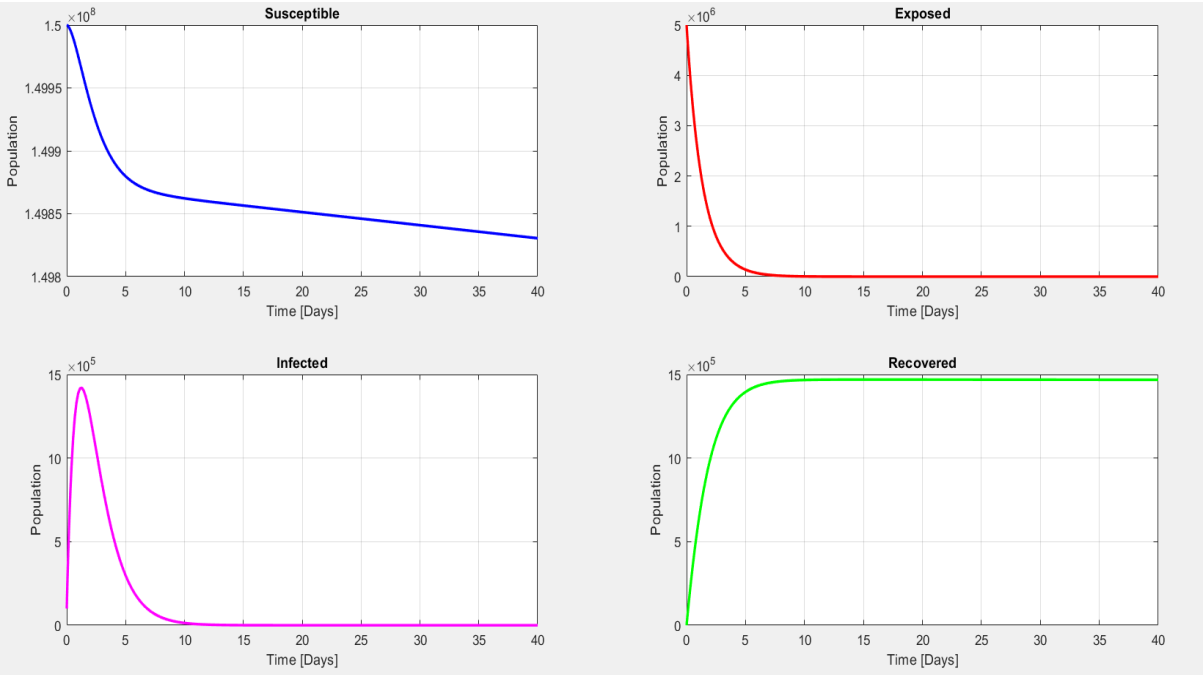

Figure 8: Dynamics of the compartments for the values of the control parameter $\eta = 1.0$ and $\gamma = 1.0$ with$R_0 = 0.08$.

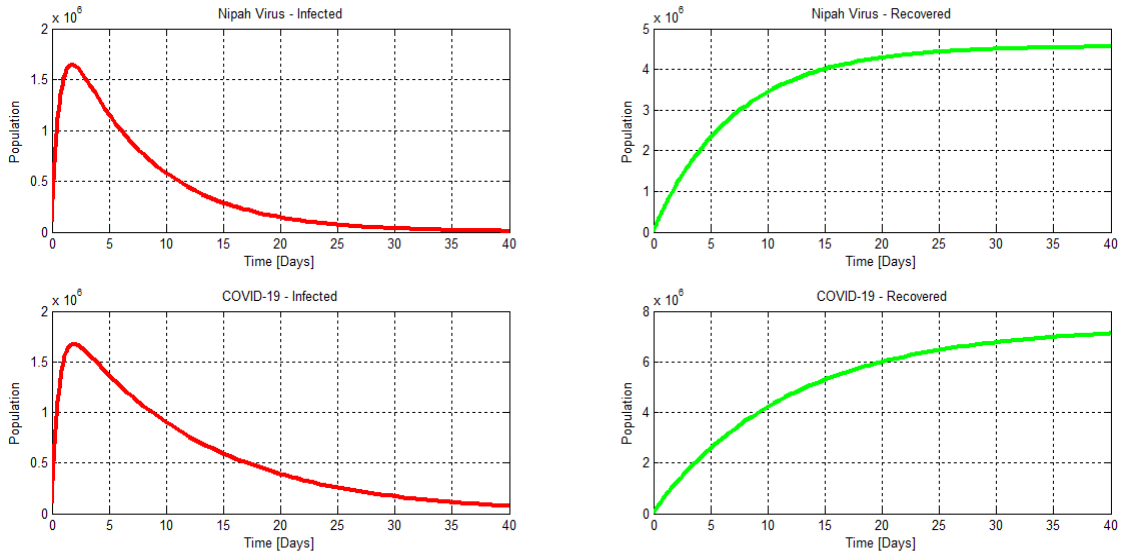

Figure 9: Sensitivity analysis of Nipah and COVID-19 under various control parameters.

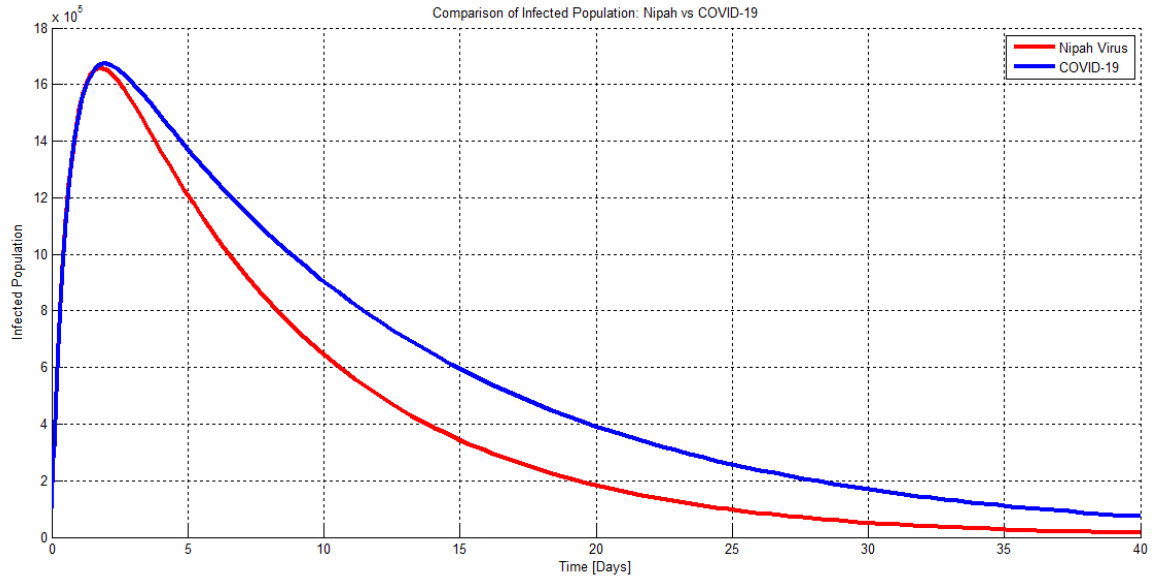

Figure 10: Sensitivity analysis of Nipah and COVID-19 under various control parameters.

The sensitivities of the control parameters also affect the basic reproduction number, R_0 . It can be observed that higher values of the control parameters lead to a reduction in the basic reproduction number.Moreover, as shown in Figures 9 and 10, the Nipah virus spreads more quickly than COVID-19. However, the recovery period for COVID-19 is longer than that for the Nipah virus. This highlights the significant role of control measures in managing the transmission and recovery processes of these diseases

5. Conclusion

We have developed a unified control model for the transmission of NiV and COVID-19. The progression of the disease outbreak is influenced by various control parameters, but we primarily focus on two: the number of quarantined individuals and the improvement in personal hygiene due to public enlightenment programs.

Our findings strongly suggest that increasing the number of quarantined individuals and enhancing personal hygiene can significantly reduce the spread of the disease in the shortest possible time. The key conclusion from our results is that higher values of these control parameters can effectively lower the basic reproduction rate.

Furthermore, as depicted in Figures 9 and 10, we observed that the Nipah virus spreads more rapidly than COVID-19. However, the recovery time for COVID-19 is longer compared to the Nipah virus. This underscores the critical impact of control measures in managing the transmission and recovery dynamics of these diseases.

This research provides valuable insights into the control of infectious diseases and can be instrumental in guiding public health strategies for managing future outbreaks. By understanding the dynamics of disease spread and the effectiveness of control measures, policymakers and health professionals can better prepare for and mitigate the impact of potential epidemics and pandemics.

Refrences

[1] Ang, B. S. P., Lim, T. C. C., & Wang, L. (2018). Nipah virus infection. Journal of Clinical Microbiology, 56(6), e01875-17.
[2] Chua, K. B., Koh, C. L., Hooi, P. S., Wee, K. F., Khong, J. H., Chua, B. H., ... & Lam, S. K. (2002). Isolation of Nipah virus from Malaysian Island flying-foxes. Microbes and Infection, 4(2), 145-151.
[3] Tan, C. T., & Wong, K. T. (2003). Nipah encephalitis outbreak in Malaysia. Annals of the Academy of Medicine, Singapore, 32(1), 112-117.
[4] Luby, S. P., Gurley, E. S. & Hossain, M. J. (2009). Transmission of human infection with Nipah virus. Clinical Infectious Diseases, 49(11), 1743-1748. Plotkin, S.A., Orenstein, W.A., Offit, P.A. Vaccines. Elsevier, 2018.
[5] World Health Organization. (2020). WHO Director-General's opening remarks at the media briefing on COVID-19, 11 March 2020. Retrieved from https://www.who.int/ (Accessed 05 June 2024)
[6] Diekmann, O., Heesterbeek, J. A. P., & Britton, T. (2013). Mathematical Tools for Understanding Infectious Disease Dynamics. Princeton University Press.
[7] Hethcote, H. W. (2000). The mathematics of infectious diseases. SIAM review, 42(4), 599-653.
[8] Looi, L. M., & Chua, K. B. (2007). Lessons from the Nipah virus outbreak in Malaysia. Malaysian Journal of Pathology, 29(2), 63. Keeling, M.J., Rohani, P. Modeling Infectious Diseases in Humans and Animals. Princeton University Press, 2008.
[9] Chua, K. B., Koh, C. L., Hooi, P. S., Wee, K. F., Khong, J. H., Chua, B. H., & Lam, S. K. (2002). Isolation of Nipah virus from Malaysian Island flying-foxes. Microbes and Infection, 4(2), 145-151.
[10] Kucharski, A. J., Russell, T. W., Diamond, C., Liu, Y., Edmunds, J., Funk, S., & Eggo, R. M. (2020). Early dynamics of transmission and control of COVID-19: a mathematical modelling study. The Lancet Infectious Diseases, 20(5), 553-558.
[11] Luby, S. P., Gurley, E. S., & Hossain, M. J. (2009). Transmission of human infection with Nipah virus. Clinical Infectious Diseases, 49(11), 1743-1748.
[12] Fong, M. W., Gao, H., Wong, J.Y., Xiao, J., Shiu, E. Y., Ryu, S., & Cowling, B.J. (2020). Nonpharmaceutical measures for pandemic influenza in nonhealthcare settings social distancing measures. Emerging infectious Disease, 26(5), 976..
[13] Morawska, L., & Cao, J. (2020). Airborne transmission of SARS-CoV-2: The world should face the reality. Environment International, 139, 105730.
[14] Kermack, W. O., & McKendrick, A. G. (1927). A contribution to the mathematical theory of epidemics. Proceedings of the Royal Society of London. Series A, Containing Papers of a Mathematical and Physical Character, 115(772), 700-721.
[15] Biswas MHA. AIDS epidemic worldwide and the millennium development strategies: a light for lives. HIV AIDS Rev. 2012;11: 87-94
[16] Biswas MHA, Paiva LT, de Pinho MDR. A SEIR model for control of infectious diseases with constraints. Math Biosci Eng. 2014;11:761-784.
[17] Daszak P, Plowright R, Epstein JH The emergence of Nipah and Hendra virus: pathogen dynamics across a wildlife-livestockhuma continuum In: Collinge S, Ray C, editors. Disease ecology. Oxford: Oxford University Press; 2006. p. 186-201 .

[18] Rajan kumar Dubey, Rajesh Pandey, (2023), A SIQRV Mathematical Model on COVID-19 Investigating the Combined Effect of Vaccination and Lockdown to Control the Spread of COVID-19. International journal of food and nutritional sciences, Volume 12, 2835-2850.
[19] Rajan Kumar Dubey and Rajesh Pandey, (2024), Analyzing Vaccine Efficacy: Stability Analysis of SEIR Model for Nipah Virus in India and Nepal. Tuijin Jishu/Journal of Propulsion Technology Vol(45), 2.
[20] Rajan Kumar Dubey and Rajesh Pandey, (2024), A mathematical model on COVID-19 studying the efficacy of testing to control the epidemic. Obstetrics and Gynaecology Forum Vol(5).
[21] https://www.worldometers.info/world-population/bangladesh-population (Accessed 05 June 2024).
[22] https://www.worldometers.info/world-population/india-population (Accessed 05 June 2024).
[23] Mithun Kumar Mandal, Muhammad Hanif and Md. Haider Ali Biswas, (2017), mathematical analysis for controlling the spread of Nipah virus infection. International journal of Modelling and simulation.
[24] https://www.macrotrends.net/global-metrics/countries/BGD/bangladesh/death-rate (Accessed 05 June 2024).
[25] https://www.worldometers.info/coronavirus/country/india/ (Accessed 05 June 2024).
[26] Zhifeng Wang and Dongmei Wang, (2021), The influence and enlightenment of five public health emergencies on public psychology since the new century: A systematic review, International Journal of Social Psychiatry, vol. 67, no. 7.
[27] https://www.ncbi.nlm.nih.gov/pmc (Accessed 05 June 2024).